Pergamon

Tetrahedron, Vol. 52, No. 47, pp. 14841-14854, 1996

0040-4020/96 $15.00 + 0.00

PII: S0040-4020(96)00915-5

Hydrolysis of Cyclic Orthoesters: Experimental Observations and Theoretical Rationalization

Shigui Li,[1] Yves L. Dory,[2]* and Pierre Deslongchamps[1]*

[1]Laboratoire de synthèse organique, [2]Laboratoire de modélisation moléculaire,
Département de chimie, Faculté des sciences, Université de Sherbrooke, Sherbrooke (Québec), Canada J1K 2R1

Abstract: Reaction products using labelled water (H_2O^{18}) and the relative rate of hydrolysis of the four bicyclic orthoesters **1-4** having a six or a seven-membered orthoester ring are reported. With the help of theoretical calculations (semi-empirical AM1 and *ab initio* 3-21G level), the results are explained by taking into account proton affinities as well as steric and stereoelectronic effects.

INTRODUCTION

The mild acid hydrolysis of orthoesters is a powerful technique to verify the principle of stereoelectronic control in the cleavage of tetrahedral intermediates.[1-3] This was further confirmed recently by a reinvestigation of the hydrolysis of tricyclic orthoesters by means of molecular modeling.[4]

Recent studies[5] on the acid hydrolysis of a bridged tricyclic acetal demonstrated that the synperiplanar oxygen lone pair arrangement is as good as the antiperiplanar one to expel a leaving group. Orthoesters have three gem oxygen atoms ready to be protonated (Scheme 1). Thus, on protonation of one of the three oxygen atoms (atom 2) and according to the (*syn* [5] or *anti*) periplanar hypothesis, C_1—O_2 bond cleavage occurs if and only if two lone pairs (one from each unprotonated oxygen) are either *syn* or *anti* periplanar to the cleaving bond. These geometrical requirements can be matched in conformer B having one *syn* and one *anti* lone pairs and in conformer C with two *anti* lone pairs. In contrast conformer A which has only one *anti* lone pair cannot undergo hydrolysis.

We wish to report a new investigation dealing with the hydrolysis of the bicyclic orthoesters **1-4** (6-6 and 6-7 *trans* fused ring systems) (Scheme 2) which brings further evidence for the above hypothesis.

CHEMISTRY

The orthoesters **1**, **2**, and **3** were synthesized by transesterification of *trans*-1,2-bishydroxymethyl cyclohexane with trimethyl orthoformate, trimethyl orthoacetate and trimethyl orthobenzoate respectively. In the same way, the orthoacetate **4** was obtained from *trans*-2-hydroxymethyl-cyclohexanol and trimethyl orthoacetate.

Pierre Deslongchamps: *FAX:* (819) 821-7910. *E-MAIL:* dlnchamp@structure.chimie.usherb.ca

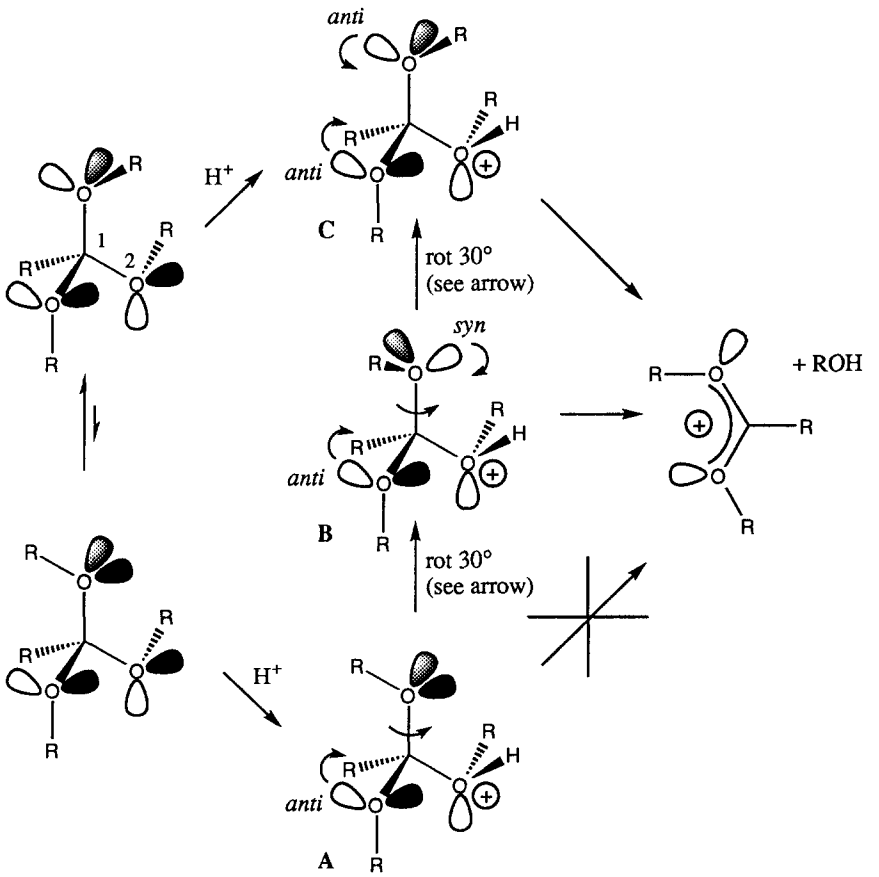

Scheme 1

RESULTS and DISCUSSION

The hydrolysis experiments starting from the orthoesters **1-4** were all performed in deuterated acetonitrile/D_2O mixtures (4:1) and catalyzed with hydrochloric acid (Scheme 2).

A study on the comparative rate of hydrolysis of **2-4** showed that the orthoacetate **2** was hydrolyzed 40 times faster than the orthobenzoate **3** whereas the orthoacetate **4** hydrolysis was 1680 fold faster than that of **3**. As regards to the products distribution, the orthoformate **1** led to a mixture (2:1) of the formate **5** and the diol **6**. The result is identical for the orthoacetate **2** leading to a mixture (2:1) of the acetate **7** and the same diol **6**. These two cases (**1** and **2**) are assumed to be entirely identical and the following discussion will consider the hydrolysis of the orthoacetate **2** only. On the contrary, the orthobenzoate **3** yields the benzoate **8** only with no trace of the corresponding diol. This last result compares with the hydrolysis of the orthoacetate **4** affording only the two possible acetates **9** and **10** (1:1 mixture), no diol being formed.

Relative rates	Starting Materials	Products
/	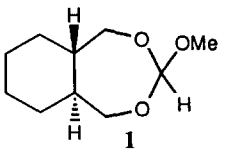 **1**	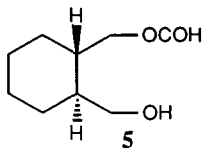 **5** 2:1 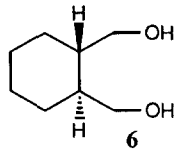 **6**
40	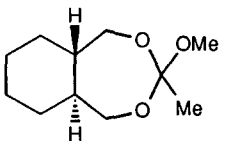 **2**	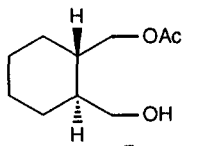 **7** 2:1 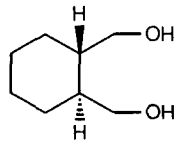 **6**
1	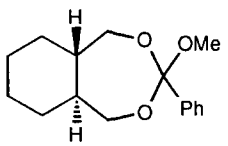 **3**	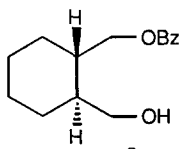 **8**
1680	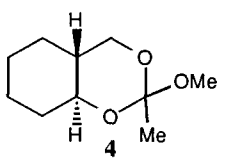 **4**	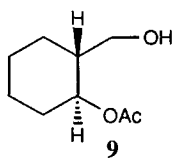 **9** 1:1 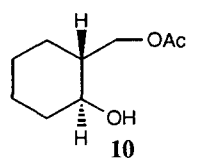 **10**

Scheme 2. Hydrolysis experiment results and comparative rates of reaction ($MeCN:D_2O$, 4:1, and catalytic HCl).

In order to understand the mechanisms of hydrolysis leading to the various products and since several competing routes may be involved (Scheme 3), hydrolysis experiments with labelled water (H_2O^{18}) have been carried out with the orthoesters **2** and **3**.

These orthoesters **2** and **3** can be in principle protonated at two oxygen positions: the exocyclic atom O-2 or the endocyclic atom O-3 (or O-4). Protonation at position 2 yields methanol and the cyclic cation **12** (R = Me or Ph) which is subsequently attacked with labelled water giving **14** (R = Me or Ph) then the labelled ester **7*** or **8***. On the contrary, protonation at one of the endocyclic oxygen induces ring opening to afford the cation **11** (R = Me or Ph). Labelled water may now attack this cation in two ways: either in an SN_2 fashion on the methoxy carbon (H_3C—O-2) leading to the ester **7** (or **8**) or directly at the central carbon atom position C-1. In the latter case, the intermediate **13** (R = Me or Ph) can be protonated at the oxygen atom O-4 to form the diol **6**; protonation can also take place at position O-2 yielding the previously described ester **7*** (or **8***).

The experimental work shows that the orthoester **2** (R = Me) was indeed producing all three products **6**, **7** and **7*** when hydrolyzed in the presence of H_2O^{18}. Therefore in this case both cations **11** and **12** contribute to the products distribution. Moreover the cation **11** (R = Me) must be formed predominantly over the cyclic cation **12** (R = Me) because the labelled ester alcohol **7***, accounting for 51% of the mixture is formed via both

cations **11** and **12**. This assumption is very reasonable since the hydrolysis products **6** and **7** (49% of the mixture) can only arise from the cation **11** too.

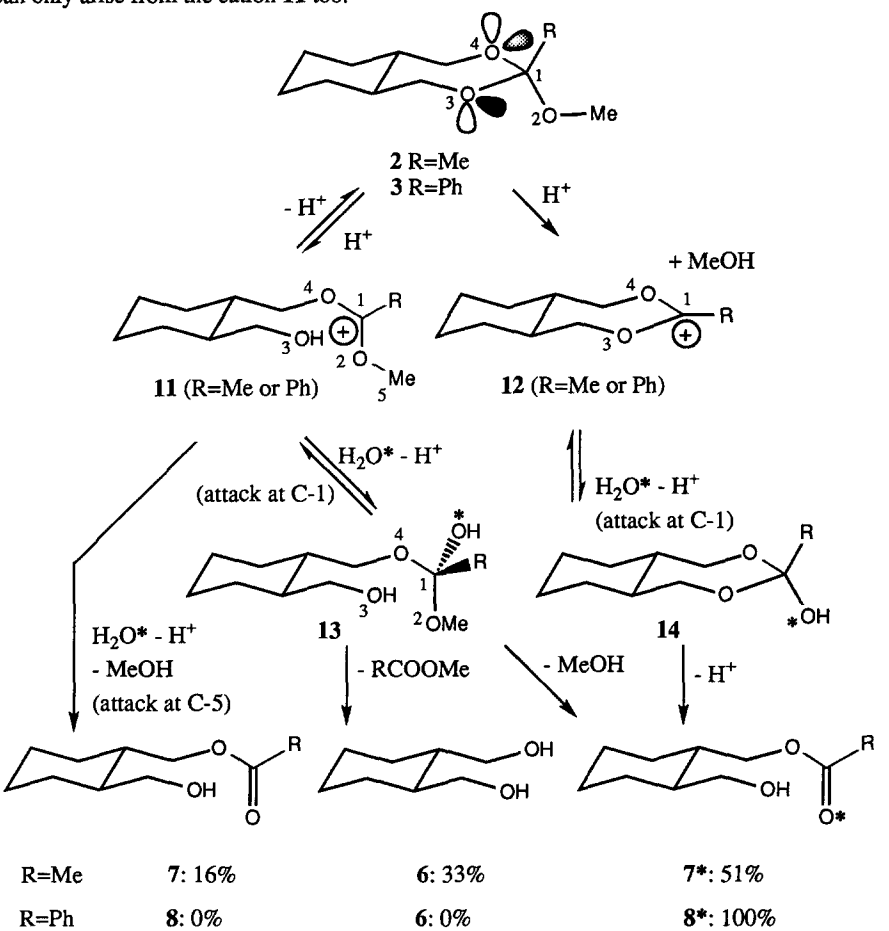

Scheme 3. Hydrolysis pathways for the orthoesters **2** and **3**.

As regards to the orthobenzoate **3** hydrolysis, the cation **11** (R = Ph) makes now no contribution to the final products distribution, the benzoate alcohol **8*** being formed only via the cyclic cation **12** (R = Ph). This assumption again is very reasonable since neither **6** nor **8** issued from **11** (R= Ph) are present.

In the case of the six-membered ring orthoester **4** hydrolysis (Scheme 4) the ester-alcohols **9** and **10** are obtained in a 1:1 ratio. Since the diol **19** is not present in the hydrolysate, it is reasonable to conclude that cations **15** and **16** do not contribute to the hydrolysis route and that the products **9** and **10** come only from the cyclic cation **17**.

In summary, all hydrolysis processes involve the cyclic cations **12** (R = Me and Ph) and **17**; whereas the cation **11** issued from seven-membered ring opening is only observed when R is a methyl substituent. These results are now rationalized in the light of stereoelectronic effects and by means of theoretical calculations.

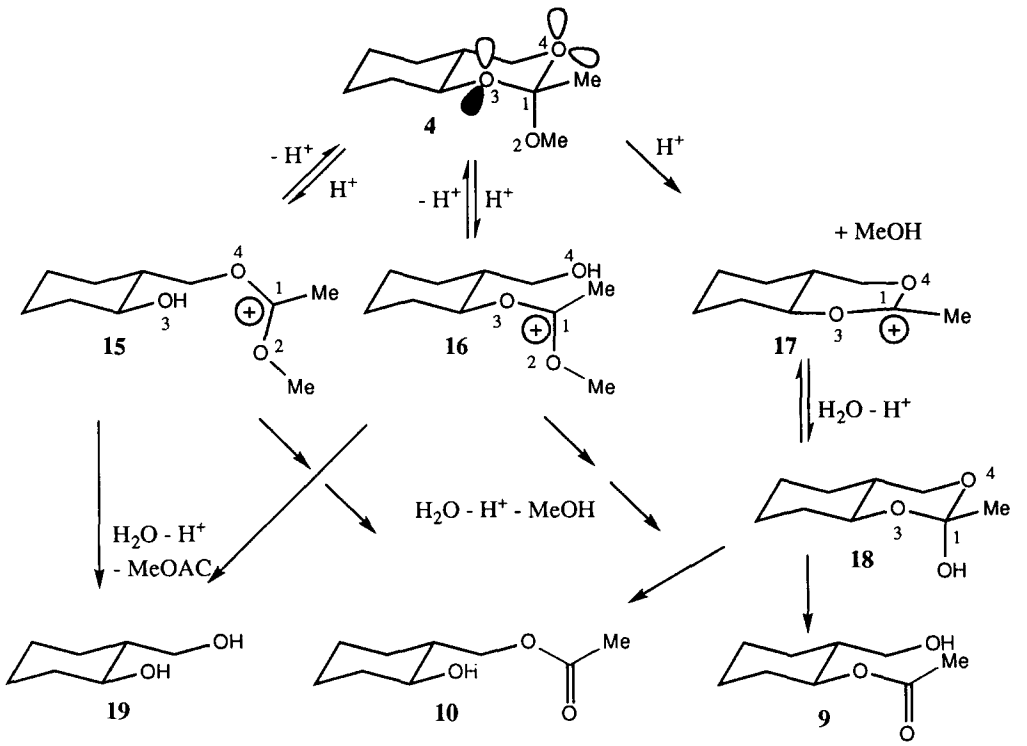

Scheme 4. Hydrolysis pathway for the orthoester **4**.

Calculations at the semi-empirical AM1 level and the ab initio 3-21G level

The orthoesters structures **2**, **3**, and **4** (axial methoxy group) were optimized using the AM1 hamiltonian.[6] For each of these compounds, two likely structures were found having simply different methoxy group orientations (Scheme 5). An X-ray picture of **3** was obtained (Figure) and matches very well the AM1 optimized structure **3b**. However the AM1 calculations predict that **3b** should be disfavored over **3a** by 1.39 kcal/mol. This apparent discrepancy may either be the result of bad AM1 parameters or come from crystal packing effects.

Nevertheless, an AM1 study of the protonated species corresponding to the neutral orthoesters **2a**, **2b**, **3a**, **3b**, **4a** and **4b**, was carried out. It was discovered that all these orthoesters once protonated undergo fragmentation without an additional energy barrier along the reaction coordinates to produce the cations **11**, **12**, **15**, **16**, and **17**. These results suggest that bond cleavage is not the rate limiting step but rather the protonation. This is in agreement with the fact that protonation is known to be playing a key role in the rate limiting step in orthoester hydrolysis.[7,8]

As a result, the transition structures corresponding to proton transfer between water and the orthoesters under study have to be located and the corresponding energies evaluated.

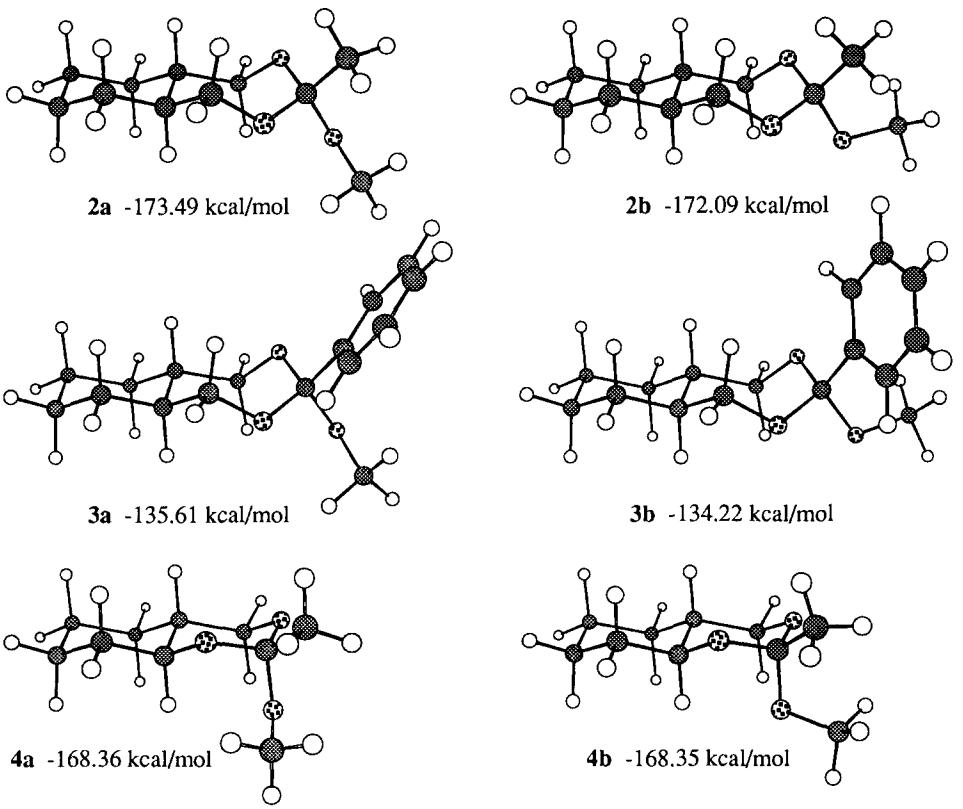

Scheme 5. AM1 optimized structures of the orthoesters **2-4**.

In order to shorten calculation times, the structures were simplified by removing the extra six-membered ring which do not actively participate in the hydrolysis reactions. Thus, the five structures **20-24** (Scheme 6, Table) were optimized at the AM1 and 3-21G[9,10] levels successively. Only one structure, **20**, was found for the six-membered ring orthoester.

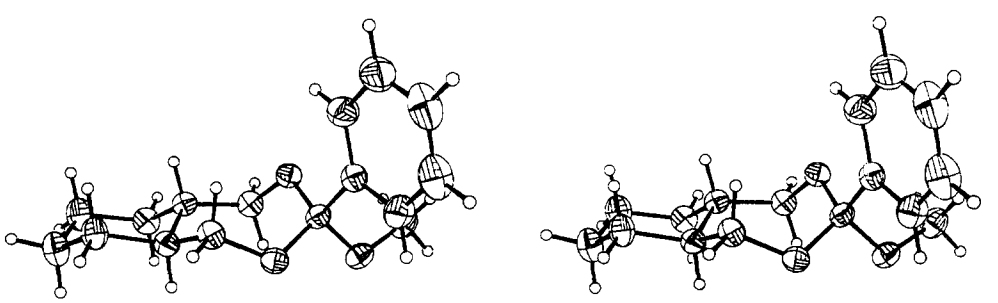

Figure. X-Ray structure of **3b**.

	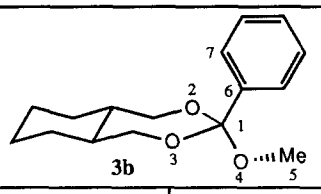 **3b**		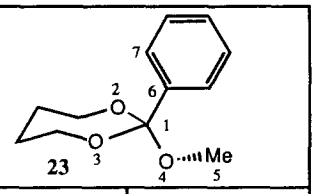 **23**	
	AM1	X-Ray	AM1	3-21G
d 1-2	1.410 Å	1.394 Å	1.410 Å	1.405 Å
d 1-3	1.415 Å	1.402 Å	1.415 Å	1.404 Å
d 1-4	1.416 Å	1.410 Å	1.415 Å	1.403 Å
d 1-6	1.510 Å	1.513 Å	1.509 Å	1.513 Å
a 2-1-3	111.38°	112.32°	111.10°	111.09°
a 2-1-4	106.96°	111.39°	106.95°	111.10°
a 3-1-4	99.31°	101.21°	99.37°	102.72°
t 2-1-4-5	71.9°	57.2°	74.3°	61.4°
t 3-1-4-5	-172.3°	176.8°	-170.2°	-179.7°
t 2-1-6-7	7.3°	12.7°	-0.1°	-3.7°
t 3-1-6-7	-117.9°	-111.4°	-125.1°	-125.9°

Table. Geometrical comparisons of structures **3b** and **23** calculated and obtained by X-ray crystallography.

In the case of the seven-membered ring orthoacetate, the two structures **21** and **22** were found, the latter being favored by AM1 and 3-21G by 1.41 kcal/mol and 1.84 kcal/mol respectively. The seven-membered ring orthobenzoate can exist either as conformer **23** (preferred 3-21G structure) or conformer **24** (preferred AM1 structure). It is worth noting that **23** corresponds to the geometry of **3b** also found in the X-ray structure of **3** (Figure). Both optimization methods are in fair geometrical agreement with the X-ray data (Table).

These structures were used as the basis to study protonation. Each orthoester having three oxygen atoms, six positions (labelled **a-f**) are available for proton delivery by H_3O^+, yielding in principle six transition structures per orthoester. All these possible sites of protonation were studied by means of the AM1 semi-empirical hamiltonian. Nevertheless, it was found that for obvious steric reasons some oxygen lone pairs could not be attacked by H_3O^+ without concomitant rotation of the methoxy group to relieve unfavorable interactions. Thus, protonation of the orthoester **20** at the *endo* position **c** was equivalent to protonation at position **e** (the other equivalent positions are indicated in Scheme 6). In the case of the six-membered orthoester **20** where all the bonds are staggered, use of the antiperiplanar lone pair hypothesis allows straightforward identification of the most basic oxygen atoms[11]. The oxygen atom O_1 receives two contributions from the lone pairs **d** and **f**, whereas its lone pair **a** only is able to donate electrons. It is therefore O_1 which should be the most protonable oxygen atom of the orthoester **20**. Indeed oxygen O_2 receives two contributions as well from **a** and **e** but it also donates electrons from both its lone pairs **c** and **d**. As regards to O_3, this atom receives only from **c** whereas its two lone pairs **e** and **f** can donate electrons; as such it must be the least basic oxygen atom. These conclusions

are dramatically confirmed by calculations which show that protonation at position O_1 is indeed the most favored process; protonation at position O_2 an O_3 are disfavored by 2.56 kcal/mol and 6.30 kcal/mol respectively. These stereoelectronic considerations and calculations are in full agreement with the experimental result, because only C_4—O_1 bond cleavage is observed and is a fast process. This latter observation can also be rationalized in terms of stereoelectronic effects, because once protonated at position O_1, both lone pairs **f** and **d** (which are already partially responsible for the large basicity of the oxygen O_1) immediately provoke C_4—O_1 bond breaking without further backbone motion.

All the transition structures (apart from **20**b) calculated indicate that the geometry of the orthoester **20** is not too much altered at the transition state. This observation suggests that both protonation, the rate limiting step, and bond cleavage are distinct, despite the fact that the second step is not accompanied by a barrier on the potential energy surface, as checked by IRC[9] (intrinsic reaction coordinate) studies starting from the transition structures (no intermediates or weak ones were located between the transition structures and the products). All the orthoesters have C_4—O bond lengths in the 1.40-1.42 Å bracket. At the transition state the C_4—O bond lengths can be classified into 3 families: the C_4—O bond whose oxygen atom gets protonated has lengthened (1.44-1.48 Å), one of the remaining C_4—O bond has shrunk (1.37-1.39 Å) whereas the other one does no change (1.40-1.42 Å).

These figures clearly demonstrate that bond cleavage is far from being complete at the protonation transition state. It is also worth noting that the distance between water oxygen and H^+ is 0.202 Å shorter than the distance between orthoester **20** oxygen O_1 and H^+ in **20**a, the most favored transition structure. This proves that the proton affinity of this orthoester is greater than that of water, because it can attract H^+ with equal strength at a longer distance at the transition state level. The same trend is also observed in the case of the seven-membered ring orthoesters **21**-**24**, although to a lesser extent (0.127 Å, 0.127 Å, 0.160 Å and 0.143 Å) for **21**f, **22**c, **23**f and **24**c which are the favored protonation transition structures, likely due to a diminished proton affinity of these orthoesters compared with **20**, as experimentally confirmed by the relative rates of hydrolysis of the orthoesters **2**-**4** (Scheme 2).

All the observations made in the case of **20** can be applied in the case of the seven-membered ring orthoesters **21**-**24**. However, due to the much floppier structures of these compounds and also to the fact that *syn* periplanar lone pairs must also be at work, application of stereoelectronic principles becomes an awkward task.

The calculations show that the seven-membered ring orthoacetate gets mainly protonated in an *endo* fashion (inside the ring, **21**f and **22**c) rather than at the *exo* position (**21**b). In this case again the calculations are in good agreement with the experiments since a Boltzmann distribution of the transition states at 25°C predicts that 88% of the protonation should take place at the endocyclic oxygen positions; it is experimentally difficult to estimate accurately the amount of endocyclic protonation versus exocyclic protonation, but at least 49% of the protonation should be endocyclic, according to the final products distribution.

In the case of the seven-membered ring orthobenzoate, the exocyclic protonation is predicted to be more favored (27%) than for the orthoacetate. Despite the large apparent difference between the experiment and the calculations, the trend (more *exo* protonation) is correctly foreseen. There also exists a major difference between orthoacetates and orthobenzoates in that the cations formed after endocyclic protonation and ring cleavage in the case of the orthobenzoate lead to structures extremely unfavorable to water attack at the cental carbon position.

		ΔHf (kcal/mol)	calc ratio		exp ratio	O----H^+----OH_2 (Å)
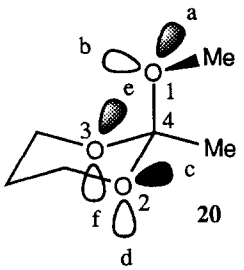	a	-40.01	98%	*exo:* 98%	100%	1.336 - 1.134
	b	(-40.31)*	-			-
	c	**20**e	-			-
	d	-37.76	2%	*endo:* 2%	0%	1.401 - 1.112
	e	-34.02	0%			1.401 - 1.112
	f	**20**d	-			-
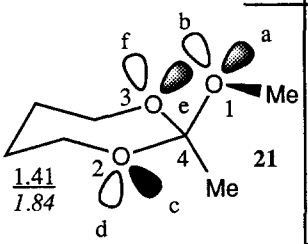	a	-47.81	3%	*exo:* 12%	< 51%	1.191 - 1.236
	b	-48.27	7%			1.265 - 1.171
	c	**22**c	-			-
	d	**22**c	-			-
	e	-44.52	0%			1.162 - 1.270
	f	-49.66	76%			1.287 - 1.160
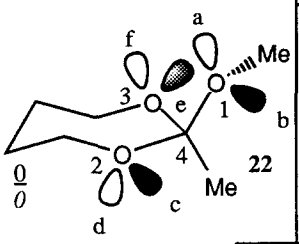	a	-47.55	2%	*endo:* 88%	> 49%	1.263 - 1.177
	b	-45.68	0%			1.244 - 1.188
	c	-48.55	12%			1.287 - 1.160
	d	**22**c	-			-
	e	**22**e	-			-
	f	**22**f	-			-
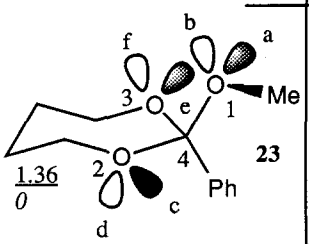	a	-12.22	10%	*exo:* 27%	100%	1.276 - 1.164
	b	-12.02	7%			1.308 - 1.147
	c	**23**d	-			-
	d	-3.09	0%			1.390 - 1.113
	e	-9.44	0%			1.193 - 1.236
	f	-13.09	42%			1.309 - 1.149
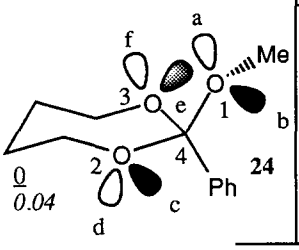	a	-12.15	9%	*endo:* 73%	0%	1.243 - 1.200
	b	-10.69	1%			1.272 - 1.169
	c	-12.98	31%			1.299 - 1.156
	d	-3.12	0%			1.400 - 1.109
	e	**23**e	-			-
	f	**23**f	-			-

Scheme 6

AM1 protonation transition structures characteristics and corresponding heats of formation (ΔHF). Relative energies of the neutral species are indicated on the left (kcal/mol; underlined: AM1, italics: 3-21G optimized including ZPE). * This structure has a boat conformation and may be disfavored in a bicyclic system.

For obvious steric reasons the plane of the phenyl is nearly perpendicular (49° and 65° in the cases of the cations issued from **23f** and **24c** respectively) to the plane defined by the 2 oxygens and their intercalated carbon (Scheme 7). This carbon is the preferred site of attack by nucleophiles, for which the best incoming trajectory is also perpendicular to the O—C—O plane.

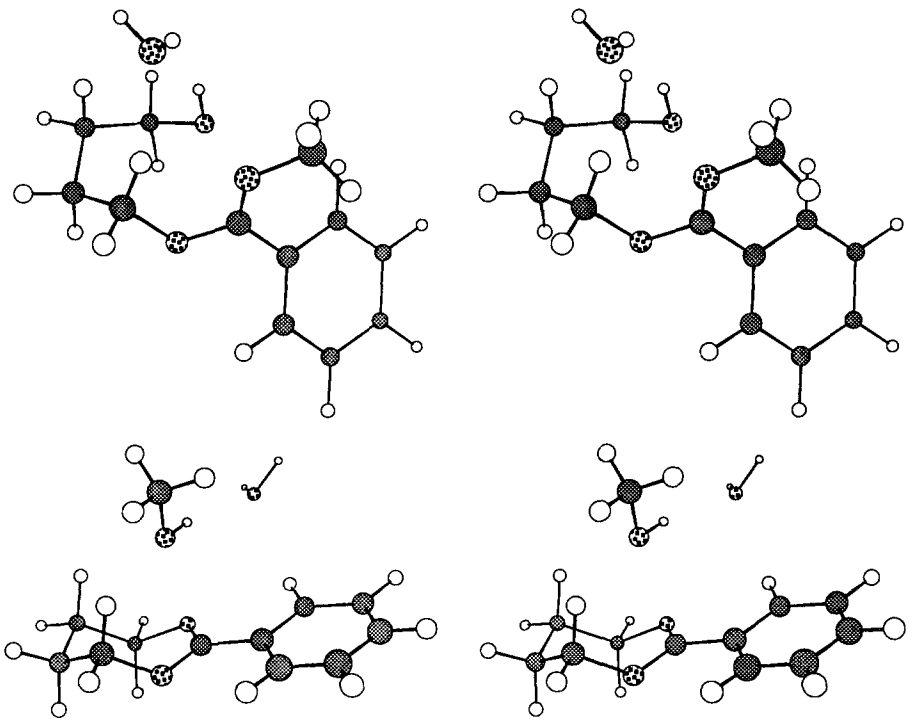

Scheme 7. Cation from **23f** (top). Cation from **23a** (bottom).

Clearly, the preferential phenyl orientation is incompatible with nucleophilic attack by water (Scheme 8) and ring closure, an intramolecular process, is much preferred leading back to the original orthobenzoate compound.

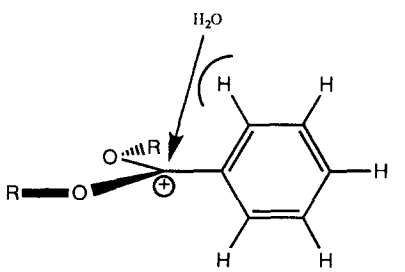

Scheme 8

Obviously, this steric hindrance to water attack on the cation is not encountered after exocyclic protonation and cleavage of the orthobenzoate since the phenyl ring become nearly coplanar with the O—C—O plane (0° in the case of the cation issued from **23**a) leaving both sides of the O—C—O plane completely free to nucleophilic attack. All these considerations dealing with the orientation of the phenyl ring become irrrelevant when the phenyl substituant is replaced by a methyl group and in the case of the orthoacetate, protonation is the only factor influencing the product distribution. In that case, the protonation transition state calculations fit perfectly with the experiment.

CONCLUSION

From the experimental data collected for the hydrolysis of the orthoesters **2**, **3** (Scheme 3), and **4** (Scheme 4) and with the help of theoretical calculations, it has become clear that these processes are controlled by stereoelectronic effects as well as by steric factors.

The neutral orthoacetate **2** has two lone pairs on the ring oxygens ready to eject methanol on protonation of the exocyclic methoxy group, one of the lone pairs being antiperiplanar to the bond undergoing cleavage and the other lone pair being synperiplanar (Schemes 3 and 6). It is also possible for one of the endocyclic oxygens to get protonated, the corresponding C—OH+ bond being cleaved with the assistance of two antiperiplanar lone pairs, one from the methoxy group and another one from the remaining endocyclic oxygen atom. In this case both types of bond breaking processes (*exo* and *endo* cyclic) take place, and the protonation would be involved in the rate-limiting step in good agreement with the theory of stereoelectronic control.

On the other hand, the orthobenzoate **3** leads only to the cation **12** (R = Ph). The calculations demonstrate that endocyclic ring oxygen protonation should still be favored, although to a lesser extend as in the case of the orthoacetate **2**. However, the nucleophilic attack of water on the cation issued from the endocyclic opening **11** (R = Ph) is highly hindered, the phenyl ring being in the way of the attacking water molecule. Such is not the case for the cation **12** (R = Ph) formed after exocyclic protonation. As a result the cation **11** does not add water, it simply reverts back to the orthobenzoate **3** and the whole hydrolytic process is slowed down when compared to that of the orthoacetate **2** (40 fold factor).

Finally, the hydrolysis of the six-membered ring orthoacetate **4** is governed by stereoelectronic factors only, and the protonation would be involved in the rate limiting step as in the case of the seven-membered ring orthoacetate **2**. The hydrolysis is however much faster (42 fold factor) for **4** because two lone pairs are already properly oriented in an antiperiplanar fashion for the exocyclic oxygen to be highly basic. In the case of the seven-membered ring orthoacetate **2**, the alignment of two antiperiplanar lone pairs is not perfect for endocyclic cleavage, it is also true for the exocyclic cleavage which requires the assistance of one antiperiplanar lone pair and one *syn* periplanar lone pair. Therefore both these *endo* cyclic and *exo* cyclic cleavages necessitate backbone geometry adjustments for the oxygen atom to become sufficiently basic, but since the orbital alignments remain imperfect, the seven-membered ring orthoacetate **2** is less basic than **4**, its hydrolysis process becomes slower.

EXPERIMENTAL

The infrared (IR) spectra were taken on a Perkin-Elmer 1600 series FTIR. Nuclear magnetic resonance (NMR) spectra were recorded on a Brüker AC 300 instrument. Mass spectra (MS) were obtained on a ZAB-IF spectrometer. Flash chromatography was performed on silica gel Merck 60, 230-400 mesh.

Hydrolysis

The orthoesters (0.1 mmol) were hydrolyzed in mixtures of deuterated acetonitrile (0.4 mL) and deuterium oxide (0.1 mL) in the presence of a catalytic amount of hydrochloric acid (0.1 N). The reactions were carried out in NMR tubes and monitored by ^1H NMR.

For comparison, competitive reactions of a mixture of two orthoesters were made. The relative rates were obtained by comparing their observed first-order rate constants which were directly provided by analysis of the decrease of the integrations of OCH_3 peaks of each orthoesters against time.[12]

Synthesis

Orthoacetate 2: A mixture of *trans*-1,2-bishydroxymethyl cyclohexane (2.88 g, 20 mmol), trimethyl orthoacetate (5 mL) and *p*-toluenesulfonic acid (15 mg) was warmed to 40°C and the formed methanol was removed by distillation with a rotary evaporator under slightly reduced pressure (about 500 mmHg) during 4 h. The excess of trimethyl orthoacetate was removed and the crude product was purified by flash chromatography (hexane/ ethyl acetate/ triethylamine, 80/20/1) to give a pure solid product (3.79 g, 95%). IR ($CHCl_3$): 1448, 1160, 1048 cm^{-1}; ^1H NMR (C_6D_6): 3.96 (1H, t, J=11.0 Hz, C<u>H</u>HO), 3.38-3.21 (3H, m, C<u>H</u>$_2$O, CH<u>H</u>O), 3.23 (3H, s, OC<u>H</u>$_3$), 1.55-1.49 (2H, m, C<u>H</u>), 1.43 (3H, s, C<u>H</u>$_3$), 1.25-0.96 (6H, m, C<u>H</u>$_2$), 0.65-0.55 (2H, m, C<u>H</u>$_2$); ^{13}C NMR (C_6D_6): 115.78 ($O_3\underline{C}$), 68.59, 66.32 ($\underline{C}H_2O$), 50.47 ($O\underline{C}H_3$), 46.57, 45.78 ($\underline{C}H$), 28.63, 28.45, 26.44, 26.37 ($\underline{C}H_2$), 20.33 ($\underline{C}H_3$); MS (m/e): 185 (M^+ - CH_3), 169 (M^+ - OCH_3).

Orthobenzoate 3: The orthobenzoate **3** was prepared according to the same procedure used to prepare the orthoacetate **2** (92%). MP: 74-75°C (hexane); IR ($CHCl_3$): 3017, 1449, 1097 cm^{-1}; ^1H NMR ($CDCl_3$): 7.61-7.35 (5H, m, ph), 4.04 (1H, t, J=12.0 Hz, C<u>H</u>HO), 3.51 (1H, dd, J=11.5 and 2.5 Hz, CH<u>H</u>O), 3.38 (1H, dd, J=12.0 and 3.0 Hz, C<u>H</u>HO), 3.21 (1H, t, J=11.0 Hz, CH<u>H</u>O), 3.02 (3H, s, OC<u>H</u>$_3$), 1.79-0.76 (10H, m, C<u>H</u>, C<u>H</u>$_2$); ^{13}C NMR ($CDCl_3$): 138.35, 128.49, 127.19 (ph), 115.00 ($O_3\underline{C}$), 68.45, 66.27 ($\underline{C}H_2$), 50.60 ($O\underline{C}H_3$), 45.94, 45.37 ($\underline{C}H$), 28.32, 28.22, 26.18, 26.04 ($\underline{C}H_2$); MS (m/e): 231 (M^+ - OCH_3), 185 (M^+ - C_6H_5).

Orthoformate 1: The orthoformate **1** was prepared according to the same procedure used to prepare the orthoacetate **2** (90%). IR (film): 1447, 1204, 1132, 1098 cm^{-1}; ^1H NMR (C_6D_6): 5.29 (1H, s, C<u>H</u>), 4.00 (1H, t, J=11.0 Hz, C<u>H</u>HO), 3.43 (1H, dd, J=12.0 and 3.0 Hz, CH<u>H</u>O), 3.33-3.24 (2H, m, C<u>H</u>$_2$O), 3.20 (3H, s, OC<u>H</u>$_3$), 1.51-0.54 (10H, m, C<u>H</u>, C<u>H</u>$_2$); ^{13}C NMR (C_6D_6): 113.28 ($O_3\underline{C}$), 69.10, 65.49 ($O\underline{C}H_2$), 52.73($O\underline{C}H_3$), 46.46, 45.61 ($\underline{C}H$), 28.50, 26.41, 26.28 ($\underline{C}H_2$); MS (m/e): 187 (MH^+), 155 (M^+ - OCH_3).

Orthoacetate 4: 2-*trans* Hydroxymethyl cyclohexanol (0.256 g, 2 mmol), trimethyl orthoacetate (1 mL) and *p*-toluenesulfonic acid (5 mg) were stirred for 28 h at room temperature. Triethylamine (2 drops) was

added and the resulting mixture was evaporated *in vacuo*, the residue was purified by flash chromatography (hexane / ethyl acetate / triethylamine, 90/10/1) to give the cyclic orthoacetate **4** (0.322 g, 92%). IR (film): 1452, 1162 cm^{-1}; ^1H NMR ($CDCl_3$): 3.72-3.64 (2H, m, C<u>H</u>, C<u>H</u>HO), 3.56 (1H, dd, J=10.5 and 4.5 Hz, C<u>H</u>HO), 3.29 (3H, s, OC<u>H</u>$_3$), 1.85-0.86 (9H, m, C<u>H</u>, C<u>H</u>$_2$), 1.45 (3H, s, C<u>H</u>$_3$); ^{13}C NMR ($CDCl_3$): 112.31 (O_3<u>C</u>), 72.81 (<u>C</u>HO), 64.43 (<u>C</u>H$_2$O), 50.29 (O<u>C</u>H$_3$), 39.76 31.20, 25.88, 24.99, 24.53 (<u>C</u>H, <u>C</u>H$_2$), 22.46 (<u>C</u>H$_3$); MS (m/e): 186 (M^+), 171 (M^+ - CH_3), 155 (M^+ - OCH_3).

Hydroxy acetate 7: The orthoacetate **2** (5.0 g, 25 mmol) was hydrolyzed in a mixture of acetonitrile (20 mL), water (5 mL) and aqueous hydrochloric acid (1 N, 2 mL) for 3 h at room temperature. The reaction mixture was neutralized with saturated sodium bicarbonate (pH about 6-7). The solvent was removed *in vacuo*, the residue was purified by flash chromatograpy (hexane/ethyl acetate, 2/3) to give the acetate **7** (2.9 g, 62%) and the diol **6** (1.09 g, 30%). IR (film): 3419, 1717, 1274 cm^{-1}; ^1H NMR ($CDCl_3$): 4.13 (1H, dd, J=11.0 and 4.5 Hz, C<u>H</u>HO), 3.98 (1H, dd, J=11.0 and 6.0 Hz, CH<u>H</u>O), 3.62 (2H, br, C<u>H</u>$_2$OH), 2.05 (3H, s, C<u>H</u>$_3$), 1.80-1.12 (10H, m, C<u>H</u>, C<u>H</u>$_2$); ^{13}C NMR ($CDCl_3$): 171.22 (<u>C</u>O), 67.60, 67.53 (<u>C</u>H$_2$), 41.91, 38.31(<u>C</u>H), 29.69, 29.37, 25.68, 25.59 (<u>C</u>H$_2$), 20.87 (<u>C</u>H$_3$); MS (m/e): 187 (MH^+), 169 (M^+ - OH), 156 (MH^+ - OCH_3).

Hydroxy benzoate 8: The orthobenzoate **3** (80 mg, 0.3 mmol) was hydrolyzed in a mixture of acetonitrile (1.2 mL), water (0.3 mL) and hydrochloric acid (0.1N, 15 µL) during 1 h. The mixture was then concentrated to give the benzoate **8** (75 mmg, 99%). IR (film): 3426, 1716, 1276, 1115 cm^{-1}; ^1H NMR ($CDCl_3$): 8.33-7.39 (5H, ph), 4.93 (1H, dd, J=11.0 and 4.0 Hz, C<u>H</u>HO), 4.24 (1H, dd, J=11.0 and 6.0 Hz, CH<u>H</u>O), 3.67 (2H, d, J=4.5 Hz, C<u>H</u>$_2$O), 2.24 (1H, br, O<u>H</u>), 1.97-1.44 (10H, m, C<u>H</u>, C<u>H</u>$_2$); ^{13}C NMR ($CDCl_3$): 166.69 (<u>C</u>O), 132.82, 130.20, 129.41, 128.27 (ph), 67.92, 65.43 (<u>C</u>H$_2$O), 44.85, 38.47 (<u>C</u>H), 29.87, 29.36, 25.63, 25.56 (<u>C</u>H$_2$); MS (m/e): 248 (M^+), 230 (M^+ - H_2O), 218 (M^+ - CH_2O), 143 (M^+ - C_6H_5CO).

Hydrolysis of orthoacetate **2** *and orthobenzoate* **3** *in* ^{18}O*-labelled water*

The orthoacetate **2** (100 mg, 0.5 mmol) was hydrolyzed in acetonitrile (3 mL) containing ^{18}O-labelled water (0.04 mL, 2 mmol) and a catalytic amount of trifluoroacetic acid. Three products, the ^{18}O-labelled hydroxy acetate **7***, the hydroxy acetate **7** and the diol **6** were obtained in a ratio of 51/16/33.

The orthobenzoate **3** (65 mmg, 0.25 mmol) was hydrolyzed in acetonitrile (2 mL) containing ^{18}O-labelled water (0.02 mL, 1 mmol) and a catalytic amount of trifluoroacetic acid. Only the ^{18}O-labelled hydroxy benzoate **8*** (100%) was obtained.

ACKNOWLEDGEMENTS

This research was supported by the Natural Sciences and Engineering Research Council of Canada (NSERCC, Ottawa) and by the "Ministère de l'Éducation" (FCAR, Québec).

REFERENCES

1. Deslongchamps, P.; Chênevert, R.; Taillefer, R.J.; Moreau, C.; Saunders, J.K. *Can. J. Chem.* **1975**, *53*, 1601.
2. Deslongchamps, P.; Lessard, J.; Nadeau, Y. *Can. J. Chem.* **1985**, *63*, 2485.
3. Deslongchamps, P.; Guay, D.; Chênevert, R. *Can. J. Chem.* **1985**, *63*, 2493.
4. Deslongchamps, P.; Dory, Y.L.; Li, S. *Heterocycles* **1996**, *42 (2)*, 617.
5. Li, S.; Kirby, A.J.; Deslongchamps, P. *Tetrahedron Lett.* **1993**, *34*, 7757.
6. Dewar, M.J.S.; Zoebisch, E.G.; Healy, E.F.; Stewart, J.J.P. *J. Am. Chem. Soc.* **1985**, *107*, 3902.
7. Bunton, C.A.; De Wolfe, R.H. *J. Org. Chem.* **1965**, *30*, 1371.
8. R. Eliason and M.M. Kreevoy. J. Am. Chem. Soc. **1978**, *100*, 7037.
9. Schmidt, M.W.; Baldridge, K.K.; Boatz, J.A.; Elbert, S.T.; Gordon, M.S.; Jensen, J.H.; Koseki, S.; Matsunaga, N.; Nguyen, K.A.; Su, S.J.; Windus, T.L.; Dupuis, M.; Montgomery, J.A. *J. Comput. Chem.* **1993**, *14*, 1347.
10. Computational procedure: All the calculations were done at the RHF level using MOPAC 6.00 (Stewart, J.J.P. QCPE No. 455) in the case of AM1 optimization and GAMESS for 3-21G calculations. The ground state structures were characterized by zero imaginary frequency and the transition state structures by only one imaginary frequency. The IRC studies were carried out with AMPAC 5.0 (Semichem, 7128 Summit, Shawnee, KS 66216).
11. Deslongchamps, P. In *Stereoelectronic Effects in Organic Chemistry*, Baldwin, J. E., Ed.; Organic Chemistry Series, Vol. I; Pergamon Press: Oxford, England, 1983. p. 31.
12. Li, S.; Deslongchamps, P. *Tetrahedron Lett.* **1994**, *353*, 5641.

(*Received in Belgium* 29 *April* 1996; *accepted* 4 *October* 1996)